J Forensic Sci, Mar. 2003, Vol. 48, No. 2
Paper ID JFS2002166_482
Available online at: www.astm.org

Michael J. Thali,[1,2,3] M.D.; Kathrin Yen,[1] M.D.; Wolf Schweitzer,[1] M.D.; Peter Vock,[2] M.D.; Chris Boesch,[4] M.D., Ph.D.; Christoph Ozdoba,[3] M.D.; Gerhard Schroth,[3] M.D.; Michael Ith,[4] Ph.D.; Martin Sonnenschein,[2] M.D.; Tanja Doernhoefer,[2] M.D.; Eva Scheurer,[1] M.D.; Thomas Plattner,[1] M.D.; and Richard Dirnhofer,[1] M.D.

Virtopsy, a New Imaging Horizon in Forensic Pathology: Virtual Autopsy by Postmortem Multislice Computed Tomography (MSCT) and Magnetic Resonance Imaging (MRI)—a Feasibility Study*

ABSTRACT: Using postmortem multislice computed tomography (MSCT) and magnetic resonance imaging (MRI), 40 forensic cases were examined and findings were verified by subsequent autopsy. Results were classified as follows: (I) cause of death, (II) relevant traumatological and pathological findings, (III) vital reactions, (IV) reconstruction of injuries, (V) visualization. In these 40 forensic cases, 47 partly combined causes of death were diagnosed at autopsy, 26 (55%) causes of death were found independently using only radiological image data. Radiology was superior to autopsy in revealing certain cases of cranial, skeletal, or tissue trauma. Some forensic vital reactions were diagnosed equally well or better using MSCT/MRI. Radiological imaging techniques are particularly beneficial for reconstruction and visualization of forensic cases, including the opportunity to use the data for expert witness reports, teaching, quality control, and telemedical consultation. These preliminary results, based on the concept of "virtopsy," are promising enough to introduce and evaluate these radiological techniques in forensic medicine.

KEYWORDS: forensic science, forensic radiology, postmortem, computed tomography, magnetic resonance imaging, virtual autopsy, virtopsy, digital autopsy

"The sad truth is that a century after the first X-ray was introduced as evidence in a law court, there is no general appreciation of the extent of the radiology potential in the forensic sciences" (1). Despite having been a part of medicolegal examinations almost from its beginning, radiology is still underestimated in forensic sciences, and Brogdon's statement holds true now as then. The concept "virtopsy" was born from the desire to implement new techniques in radiology for the benefit of forensic science. The term *virtopsy* was created from the terms *virtual* and *autopsy*: "virtual" is ancient Latin for "useful"; autopsy is a combination of the Greek terms "autos" (=self or with one's own) and "opsomei" (=seeing with eyes): so "autopsy" means "seeing with one's own eyes." Because our goal was to eliminate the subjectivity of "autos," we merged the two terms virtual and autopsy—deleting "autos"—to create virtopsy. Virtopsy is meant to be an objective documentation and analysis process of physical features and evidence. There have been great improvements in multislice computed tomography (MSCT) and magnetic resonance imaging (MRI) technology, increasing both contrast and resolution and offering unparalleled possibilities of 2D and 3D reconstruction. Our aim was to establish an observer-independent, objective, and reproducible forensic assessment method using modern imaging technology, eventually leading to minimally invasive "virtual" forensic autopsy. The goal was to investigate the potential feasibility of a minimally invasive forensic autopsy using radiologic imaging techniques. Therefore, a systematic approach to evaluate the practicality and reliability of radiologic imaging techniques was performed and compared with conventional forensic methods for forensic autopsy practice.

The demands on radiological autopsy were to be identical with those of traditional medicolegal autopsy, namely to address and explain the following five forensic relevant points:

I. *Atrium mortis* (i.e., a pathophysiological reconstruction and explanation of the cause of death).
II. *Relevant forensic patho-morphologic findings* in the bones, tissues, and organs.
III. *Vital reactions* elucidating the sequence of injury and death: in forensic pathological investigations, the question whether an injury was received before or after death is often an important

[1] Institute of Forensic Medicine, University of Berne, Switzerland.
[2] Institute of Diagnostic Radiology, University of Berne, Switzerland.
[3] Department of Neuroradiology, University of Berne, Switzerland.
[4] Department of Clinical Research, Magnetic Resonance Spectroscopy, University of Berne, Switzerland.

* Supported by a grant from Gebert Ruef Foundation, Switzerland. Paper presented in part at the Meeting of the German Society of Forensic Medicine, "New Radiological Methods in Forensic Sciences," September 2001, Interlaken, Switzerland, and at the Meeting of the American Association of Forensic Science, February 2002, Atlanta, GA.
Received 7 May 2002; and in revised form 6 Aug. 2002 and 3 Oct. 2002; accepted 4 Nov. 2002; published 6 Feb. 2003.

matter. The answer to this question lies with findings that only occur with intact circulation (e.g., fatal hemorrhage, air and fat embolism, cutaneous emphysema) and respiration (e.g., aspiration). These findings are termed "forensic vital reactions."

IV. Based on Points I–III, *reconstruction of injuries* with regard to force, biomechanics, and dynamics.

V. *Recapitulation and visualization* of the atria mortis comprehensible to both laymen and experts in a court of law, thereby allowing for objective evaluation of medicolegal reports and just appreciation of a particular case.

Material and Methods

This study was approved by the responsible justice department and also the ethics committee of the University of Berne.

Case Samples

Forty deceased persons among those delivered to the Institute of Forensic Medicine for forensic autopsy were studied. Sex ratio was f = 7, m = 33; mean age at death was 46 years ranging from 6 months to 83 years. As shown in Table 1, the sample comprised 18 cases of blunt trauma (motor vehicle accidents, $n = 11$; fall from heights, $n = 4$; blunt injuries, $n = 3$); 8 gunshot wounds; 6 sudden cardiac deaths; 2 drownings; 2 knife wounds; 2 cases of strangulation; 1 electrical accident; and 1 case of sudden infant death syndrome (SIDS). In addition, we examined one suspected case of malpractice after dens fixation. One of the cadavers was burnt and another one decomposed. The manner of death was due to natural causes in $n = 6$ cases and non-natural causes in $n = 34$ Cases. The latter consisted of 3 homicide cases, 18 accidents, 12 cases of suicide, and 1 case of sudden infant death.

Imaging

Anonymity of the deceased—as requested by the ethics committee—was preserved by wrapping the corpses in artifact-free body bags. MSCT and MRI were performed at a mean of 32 h after death, with the exception of the decomposed cadaver, which was discovered after approximately three weeks.

MSCT scanning was obtained on a GE Lightspeed QX/i unit, MRI scanning on a GE 1.5 T Signa Echospeed Horizon, version 5.8 unit (General Electric Medical Systems, Milwaukee, WI). In areas of forensic importance, axial MSCT was performed with 4×1.25-mm collimation; 5-mm and 1.25-mm sections as well as sagittal and coronal reformations were calculated. Duration of the average MSCT scan after preparation was 10 to 15 min. For MRI, we used a standardized protocol and additional sequences to address specific questions. T2-weighted FSE (TR/TE 4000/90 ms) and T1-weighted SE sequences (TR/TE 400/15 to 20 ms) were systematically used. T2-weighted images of the head were obtained in all three planes and T1-weighted images in the axial plane with a slice thickness of 4 mm (3 mm for children) and gaps of 1 mm. The body and—when appropriate—extremities were scanned using the T2-weighted FSE technique with fat saturation in the coronal plane and the T1-weighted sequence in the axial plane; the slice thickness was 5 mm with gaps of 1 mm. Individual sequences were added as needed, e.g., using the same parameters in an additional plane, STIR, gradient echo, or Flaiv sequences. MRI studies usually required 2 to 3 h. Forensically important body areas were evaluated as shown in Table 2. On average, for every case two areas were examined using MSCT, 1.98 areas using MRI, and 0.68 areas were not examined radiologically. In total, about 80,000 images were acquired; 64,000 of these were CT scans and 16,000 MRI scans. Image interpretation was performed by board-certified radiologists.

Autopsy

Autopsy was performed by board-certified forensic pathologists at a mean of 46 h after death. All three body cavities (cranium, thorax, abdomen) were examined except for two cases in which opening of the skull and two further cases in which opening of the thoracic and abdominal cavity were expressly reserved by the authorities. Conventional autopsy procedure was modified according to need, i.e., forensic neck dissection was performed in cases of strangulation, additional dorsal dissection following motor vehicle accident (MVA), and drowning dissection with diatom asservation when relevant.

Correlation of Autopsy and MSCT/MRI Results

Imaging and autopsy results were compared and evaluated according to Points I–V discussed in the introduction (see Table 1).

Results

The results of MSCT/MRI and autopsy of the 40 corpses are shown in Table 1 with regard to recognition of:

1. The atrium mortis (cause of death, Figs. 1–10, 12–14).
2. Relevant forensic traumatologic findings in the bones (Figs. 1, 10), organs, and tissues (Figs. 1, 5, 8–14).
3. Vital reaction (circulatory and respiratory system, Figs. 3–9, 13).
4. The potential for forensic reconstruction (Figs. 1, 5, 11, 14).
5. Visualization (Figs. 1, 9, 11, 12, 14).

as compared with the "gold standard" of conventional forensic autopsy.

Combined findings are frequent, since parameters such as combined atria mortis or combined vital signs (circulatory and respiratory) are often used in medical and forensic data interpretation.

In our 40 forensic cases, 47 partly combined causes of death were diagnosed at autopsy and 26 (55%) causes of death were found independently using only radiological image data (see Table 1). Certain causes of death escaped detection by imaging (fatal hemorrhage, $n = 13$; cardiac failure, $n = 6$; fat embolism, $n = 2$). Radiology was superior to autopsy in revealing certain cases of cranial, skeletal, or tissue trauma; postmortem imaging of organ lesions, however, proved difficult. Forensic vital signs such as air embolism, subcutaneous emphysema, and aspiration were diagnosed equally well or better using MSCT/MRI, whereas it was not possible to document the vital signs hemorrhage and fat embolism. In cases with extensive blood loss and exsanguation, a collapse of the descending aorta by a mean of $33 \pm 5\%$ was observed at the level of the left ventricle, as compared to a collapse by $15 \pm 9\%$ in cases of cardiac death.

At least, reconstruction and visualization of the 40 forensic cases were easily feasible by using imaging techniques.

Discussion

Postmortem radiological examinations date back to the year 1898 (1), and conventional radiological imaging has since been applied in numerous ways to the fields of forensic medicine.

The spectacular rise and development of digital sectional imaging (MSCT; MRI) in recent years has allowed the conception and launching of a systematic and prospective study such as "virtopsy."

TABLE 1—*Results. Case material with circumstances, cause of death, relevant injuries, signs of vitality, and reconstruction as well as the utility of imaging.*

	Circumstances	Cause of Death	C	M	A	V	Case Relevant Injuries	C	M	A	V	Signs of Vitality	C	M	A	V	Reconstruction	V
001	suicide	air embolism	+	+	+	+	ballistic burst fracture pattern	+	−	+	+	air embolism	+	+	+	+	cerebro-cranial	+
	gunshot	hemorrhage	−	−	+	−	bullet canal through brain tissue	+	+	+	=	blood aspiration	+	+	+	=	trauma by gunshot	
	wound of the																	
	head																	
002	motor vehicle	hemorrhage	−	−	+	−	cardiac rupture	−	−	+	−	fat embolism	−	−	+	−	blunt thoracic and	=
	accident						thorax lesions	+	+	+	+						abdominal trauma	
	(MVA)–						hemothorax	+	+	+	=							
	(driver)						lesions of abdominal organs	−	−	+	−							
003	MVA–	hemorrhage	−	−	+	−	ruptured pericardium	−	−	+	−	fat embolism	−	−	+	−	impact trauma	+
	motorcycle	fat embolism	−	−	+	−	thoracic lesions	+	+	+	=							
004	MVA–	air embolism	+	+	+	+	thorax lesions	+	+	+	+	air embolism	+	+	+	+	intensity and direction	+
	burnt body	hemorrhage	−	−	+	−	intensity and sequels of heat/	+	+	+	+	blood aspiration	+	+	+	=	of heat	
							burn changes to the body					soot particles in trachea	−	−	+	−		
005	accident–	elevated ICP	+		+	=	crushed cervical spinal cord	−		+	−	air embolism	+		+	+	fall on head resulting	+
	fall from	hemorrhage	−		+	−	unilateral lung rupture	−		+	−	subcutaneous	+		−	+	in skull fracture	
	scaffolding	air embolism	+		+	+	lesions of abdominal organs	−		+	−	emphysema						
							fractures	+		+	+	fat embolism	−		+	−		
006	sudden death	myocardial infarction	−	−	+	−	myocardial infarction	−	−	+	−						no lesions–death by	=
							myocardial hypertrophy	+	+	+	=						natural causes	
							coronary sclerosis	+	−	+	−							
007	accident–	elevated ICP	+	+	+	=	skull fracture system	+	−	+	+	fat embolism	−	−	+	−	combined skull	+
	blunt trauma						brain lesion	+	+	+	=						fracture system	
	(falling tree)																	
008	MVA–	cardiac rupture	−	−	+	−	organ lesions	−	−	+	−	fat embolism	−	−	+	−	impact lesions with	+
	(victim was	cervical spinal cord	−	+	+	−	fracture patterns	+	+	+	+	traumatic pulmonary	−	−	+	−	fracture patterns	
	overrun by	rupture					tissue trauma	+	+	+	=	emphysema						
	car)																	
009	MVA–	hemorrhage	−	−	+	−	abdominal organ lesions	−	−	+	−	aspiration of gastric	+	+	+	=	overrun lesions with	−
	(victim was						blood in abdomen	+	+	+	=	contents					organ lesions	
	overrun by						hydrocephalus with CP-shunt	+	+	+	=							
	car)																	
010	suicide–	asphyxia	−	−	−	=	hyoid fracture	+	−	−	+	hemorrhage into throat	−	−	+	=	strangulation mark	+
	strangulation						hypoxia	−	−	−	=	tissues and muscles					(hanging)	
011	suicide–	brainstem hemorrhage	−	+	+	=	ballistic burst fracture pattern	+	−	+	+	air embolism	+	+	+	+	cerebro-cranial	+
	gunshot						bullet canal through brain tissue	+	+	+	=	blood aspiration	+	+	+	=	trauma by gunshot	
	wound of the																	
	head																	
012	suicide–	decerebration	+		+	=	ballistic burst fracture pattern	+		+	+	air embolism	+		+	+	cerebro-cranial	+
	gunshot	hemorrhage	−		+	−						blood aspiration	+		+	=	trauma by gunshot	
	wound of the																	
	head																	
013	sudden death	cardiac failure		−	+	−	myocardial infarction		+	+	=						no lesions–death	=
	(in hospital)						myocardial hypertrophy		+	+	=						by natural causes	
							ruptured coronary plaque		−	+	−							
014	sudden death	cardiac failure		−	−	=	myocardial hypertrophy		+	+	=						no lesions–death	=
																	by natural causes	
015	MVA–	brainstem rupture	−	+	+	=	fracture patterns	+	−	+	+	fat embolism	−	−	+	−	fracture patterns	+
	(victim was						heart pierced by fractured rib	−	−	+	−						overrun lesions	−
	overrun by						abdominal organ lesions	−	−	+	−						with organ lesions	
	car)																	
016	suicide–	elevated ICP	+	+	+	=	ballistic burst fracture pattern	+	−	+	+	fat embolism	−	−	+	−	cerebro-cranial	+
	gunshot						bullet canal through brain tissue	+	+	+	+						trauma by gunshot	
	wound,																location of projectile	+
	intracranial																	
	bullet																	
017	sudden death	cardiac failure		−	+	=	myocardial infarction		−	+	−						no lesions–death by	=
							myocardial hypertrophy		+	+	=						natural causes	
							pronounced coronary sclerosis		−	+	−							

TABLE 1—*Continued.*

	Circum- stances	Cause of Death	C	M	A	V	Case Relevant Injuries	C	M	A	V	Signs of Vitality	C	M	A	V	Reconstruction	V
018	MVA– bicyclist	cerebro-cranial lesions	+	+	+	=	skeletal lesions tissue lesions brain lesions	+ − +	− + +	+ + +	+ = +	fat embolism	−	−	+	−	impact direction	+
019	accident–fall on the head	elevated ICP secondary brainstem hemorrhage	+ −	+ +	+ +	= +	brain lesions	+	+	+	=	fat embolism	−	−	+	−	fall on the head	+
020	MVA– (driver)	tension pneumothorax air embolism	+ +	+ +	− +	+ +	fracture patterns tissue lesions	+ −	− +	+ +	= −	subcutaneous emphysema fat embolism	+ −	+ −	− +	+ −	dashboard injuries	+
021	suicide– gunshot wound, intracranial bullet	brainstem laceration	−	+	+	=	ballistic burst fracture pattern bullet canal through brain tissue	+ +	− +	+ +	+ =	air embolism (status post coronary bypass)	+	+	−	+	cerebro-cranial trauma location of projectile	+ +
022	suicide– gunshot wound of the head	brainstem laceration	−	+	+	=	ballistic burst fracture pattern bullet canal through brain tissue	+ +	− +	+ +	+ =	air embolism blood aspiration	+ +	+ +	+ +	+ =	cerebro-cranial trauma by gunshot	+
023	MVA– (driver)	air embolism aspiration hemorrhage	+ + −	+ + −	+ + +	+ = −	fractures (dens fracture) abdominal organ lesions	+ −	− +	+ +	+ −	air embolism blood aspiration traumatic pulmonary emphysema	+ + −	+ + −	+ + +	+ = −	dashboard injuries	+
024	possible SIDS	none as yet	−	−	−	=	skeletal system mucus in middle ears subdural blood film	+ + −	− + −	+ + +	+ + −	fat embolism	−	−	+	−	absence of fractures (babygram)	+
025	sudden death while swimming	cardiac failure **(arhythmia)**	−	−	+	−	myocardial hypertrophy	+	+	+	=						no lesions–death by natural causes	=
026	sudden death	cardiac failure		−	+	−	myocardial infarction myocardial hypertrophy		+ +	+ +	= =						no lesions–death by natural causes	=
027	homicide– blunt trauma to the head, advanced decay	cerebro-cranial trauma hemorrhage	+ −		+ +	+ −	fracture pattern gaseous distension, decay	+ +		+ +	+ +	fat embolism	−	−	+	−	cerebro-cranial lesions	+
028	accident–fall from roof	elevated ICP hemorrhage	+ −	+ −	+ +	= −	fracture pattern brain lesions	+ +	− +	+ +	+ =	air embolism		+	+	+	cerebro-cranial lesions	+
029	homicide– blunt trauma to the head	***hypoxia***		−	−	+	fracture pattern		+	+	+	fat embolism		−	+	−	blunt trauma to face	+
030	suicide– slashed throat	hemorrhage	−	−	+	−	slash wounds	+	+	+	−	fat embolism	−	−	+	−	cut wounds	−
031	suicide– gunshot wound of the head	air embolism	+	+	+	+	ballistic burst fracture pattern brain lesions	+ +	− +	+ +	+ =	air embolism	+	+	+	+	cerebro-cranial lesions	+

(continues)

TABLE 1—*Continued.*

032	suicide–	asphyxia	−	−	−	=	hyoid bone/ thyroid cartilage	+	−	+	+	hemorrhage in neck tissues	−	+	+	=	strangulation mark	+
	hanging						hypoxia	−	−	−	=						(hanging)	
033	homicide–	Air embolism	1		1	1	fracture pattern	1		1	1	air embolism	1		1	1	localisation of projectile	1
	gunshot to the	blood aspiration	+		+	=	bullet canal in tissue	−		+	−	blood aspiration	+		+	=	bullet canals torso	−
	trunk	hemorrhage	−		+	−	pneumothorax	+		+	+							
034	suicide–	drowning	+	+	+	=	fluid in paranasal sinuses	+	+	+	+	diatoms	−	−	+	−	localisation of	+
	death in						right ventricular failure	+	+	+	=						drowning fluid	
	bathtub						aqueous emphysema	+	+	+	=							
035	MVA–	extensive fat	−	−	+	−	skeleton lesions	+	−	+	+	fat embolism	−	−	+	−	impact direction	+
	bicyclist	embolism					tissue lesions	−	+	+	=							
							brain lesions	+	+	+	+							
036	suicide–	hemorrhage	−	−	+	−	wound canal / depth	+	+	+	=	fat embolism	−	−	+	−	wound canal / depth	=
	thorax stab																	
	wound																	
037	accident–fall	cardiac failure	−	−	−	=	fractured dens (postoperative	+	−	+	=						operation site	=
	and dens	(arhythmia)					site)											
	fracture						cerebral hypoxia	−	−	−	−							
038	accident–	cardiac failure		−	−	=	electricity marks		+	+	=						no lesions	=
	electric shock																	
039	accident–	drowning	+	+	+	=	fluid in paranasal sinuses	+	=	+	+	diatoms	−	−	+	−	localization of	+
	drowning						right ventricular failure	+	+	+	=						drowning fluid	
							aqueous emphysema	+	+	+	=							
040	MVA–	crushed cervical	−	+	+	=	fractures (including dens)	+	−	+	+	fat embolism	−	−	+	−	impact localization/	+
	pedestrian	spinal cord					cervical spinal cord lesions	−	+	+	=						direction	
							tissue lesions	−	+	+	=							

Legend:

"C" = MSCT; "M" = MRI; "A" = forensic autopsy.
Recognition of crucial forensic sign according to imaging method:
+: sign recognized by imaging.
−: sign not recognized by imaging.
"V" = validity of digital imaging results as compared to those obtained by conventional autopsy.
Comparative evaluation of "imaging vs. autopsy" with regard to ease and precision of sign recognition:
−: forensic sign not recognized by MSCT/MRI; superiority of conventional autopsy.
= : forensic sign recognized equally well by MSCT/MRI and autopsy.
+: forensic sign recognized better by MSCT/MRI; superiority of radiology/imaging.
Notice: the categories "vital signs" and "reconstruction" are unimportant in cases of cardiac death *from "natural" causes; therefore, the corresponding fields in the table are empty.*

TABLE 2—*Radiological examination of the 40 bodies.*

Examination Type	Head	Trunk	Extremities
MSCT + MRI	29	28	9
MSCT	6	6	2
MRI	2	5	6
Area not examined	3	1	23
Total	$n = 40$	$n = 40$	$n = 40$

Although either technique has already been used in particular forensic cases (2–8) as well as in systematic organ studies (9–14), "virtopsy" is, to our knowledge, the first study in which the radiological modalities MSCT and MRI are used systematically and in combination. Patriquin et al. (12) presented their preliminary clinical experience with postmortem whole-body magnetic resonance imaging as an adjunct to autopsy. They hinted that modern imaging techniques might also be of use in forensic pathology. The results of our systematic comparison support this, particularly when using MSCT and phased-array rapid sequence MRI in combination. In the following, we shall analyze and discuss our results according to five forensic relevant Points I–V (cause of death, traumatologic findings, vital reaction, reconstruction, visualization, and interpretation).

I. Cause of Death

Atrium Mortis: Brain

Similarly to clinical cases (15–17), intracerebral and ventricular hemorrhage as well as sub- and epidural hematoma and extensive subarachnoid hemorrhage were easily diagnosed by radiology; however, MRI proved relatively insensitive to minor or tiny subarachnoid hemorrhage (5).

Collapse of the cerebrospinal fluid (CSF) cushion may cause the brain to sink and rest on the occiput, a phenomenon observed in postmortem radiological imaging only and with unknown, if any, significance. Fatal brainstem lesions (Cases 008 and 015) and secondary edema following neurotrauma showed typical signs of elevated intracranial pressure (ICP) (Case 007, Fig. 1*c* and 1*d*).

Acute cerebral hypoxia as occurring in cases of strangulation (Cases 010 and 032) up to now can be diagnosed neither by imaging nor through conventional techniques if survival time is short.

Atrium Mortis: Cardiovascular System

Considering that sudden cardiac death accounts for nearly 80% of natural deaths in forensic practice, we focused our study on this pathology. Our results only partially agree with those of Patriquin et al. (12), who stated that "MRI was insensitive to ischemic changes in the cardiac muscle and provided inadequate evaluation of the coronary arteries." In two out of six cases of sudden cardiac death in our study, infarction of the myocardium was visible on MRI (Cases 013 and 026; Fig. 2*a* and 2*b*). Hsu et al. (18) have also succeeded in differentiating normal from infarcted cardiac tissue (fixed in formaline) using MRI. Differences in signal intensity in our study resembled those found in clinical cases with a signal-to-noise ratio of about 30% in T2-weighted sequences (19). Myocardial hypertrophy was easily diagnosed on MSCT and MRI in our study. Coronary sclerosis was diagnosed on MSCT (Fig. 9*a*); however, in the absence of circulation, plaque rupture and thrombosis escape postmortem detection and require further studies (20–23).

Clinically and radiologically, drowning (Cases 034 and 039) seems to produce massive engorgement of the inferior vena cava (Fig. 3*a* and 3*b*) similar to that found in right ventricular failure (24). Histological examination confirms this observation, since liver histology showed impressive acute capillary stasis as a sign of right ventricular failure.

Radiological signs of death by fatal hemorrhage still have to be defined. As long as there is no external hemorrhage, the presence of large amounts of blood in either thoracic or abdominal cavities (Cases 002 and 009) can be detected or at least hinted at by imaging. The intense pallor of internal organs characteristic of exsanguination visible at autopsy cannot as yet be detected by radiology. In cases with extensive blood loss, a collapse of the descending aorta may be a reproducible radiological sign for massive or even fatal hemorrhage (Fig. 12*d*). Diameter reduction of the aorta has been observed clinically in cases of shock (mainly in young children) (25); the collapse and loss of sphericality of vessels—documented in our study—was not described before. Following precise autopsy definition of death by hemorrhage and radiological measurements of aortic diameter at various locations, prospective studies will have to determine the reliability of this aortic collapse sign.

Atrium Mortis: Lung

The pathology of the lung is of major importance in forensic and radiological diagnosis (26,27). Discriminate imaging of the lung is of central interest in forensic radiology. In our cases inner lividity due to postmortem hypostasis (Fig. 4*a* and 4*b*) could be distinguished from lung contusion (Fig. 5) and blood aspiration (Fig. 4*a-c*) as well as from aspiration of stomach contents, which caused a particularly course pattern of bronchogenic spread and subsegmental collapse (Fig. 6).

In drowning, besides the signs of right ventricular failure (distension of the inferior vena cava and engorgement of the systemic veins), we find patchy lobular lesions (mosaic pattern) in aqueous emphysema (Fig. 7). Drowning fluid can be visualized in the sinuses and duodenum (Fig. 8*a–c*).

In the postmortem MRI study by Ros, airless lungs in stillborn infants were a sign of death before the first breath (13). This is an important sign in conventional forensic autopsy, which now can be determined by radiology, too.

Fat embolism in pulmonary vessels could not be diagnosed using the sequences and protocols applied in this study. Recognizing this important forensic evidence usually requires microscopy, but perhaps future examination methods of the virtopsy project (methods like Mirco magnetic resonance/magnetic resonance microscopy imaging) will shed new light here.

In contrast, tension pneumothorax with pulmonary collapse due to compression (Fig. 9*a* and 9*b*) is better detected by imaging, since the diagnostically and topographically important mediastinal shift will be lost once the chest cavity is opened during autopsy.

Solitary, Combined, Competing Atrium Mortis

Three pathophysiological categories of "causes of death" exist in forensic medicine. We distinguish the *solitary* (one single cause of death), the *combined* (combination of several pathophysiological processes leading to death as for example hemorrhage and aspiration), and the *competing causes of death* (simultaneously occurring lesions, each fatal in its own right, e.g., simultaneous rupture of aortic arch and brainstem).

Combined cause of death occurred for example in Cases 023 and 033 in which imaging revealed both air embolism and aspiration. In

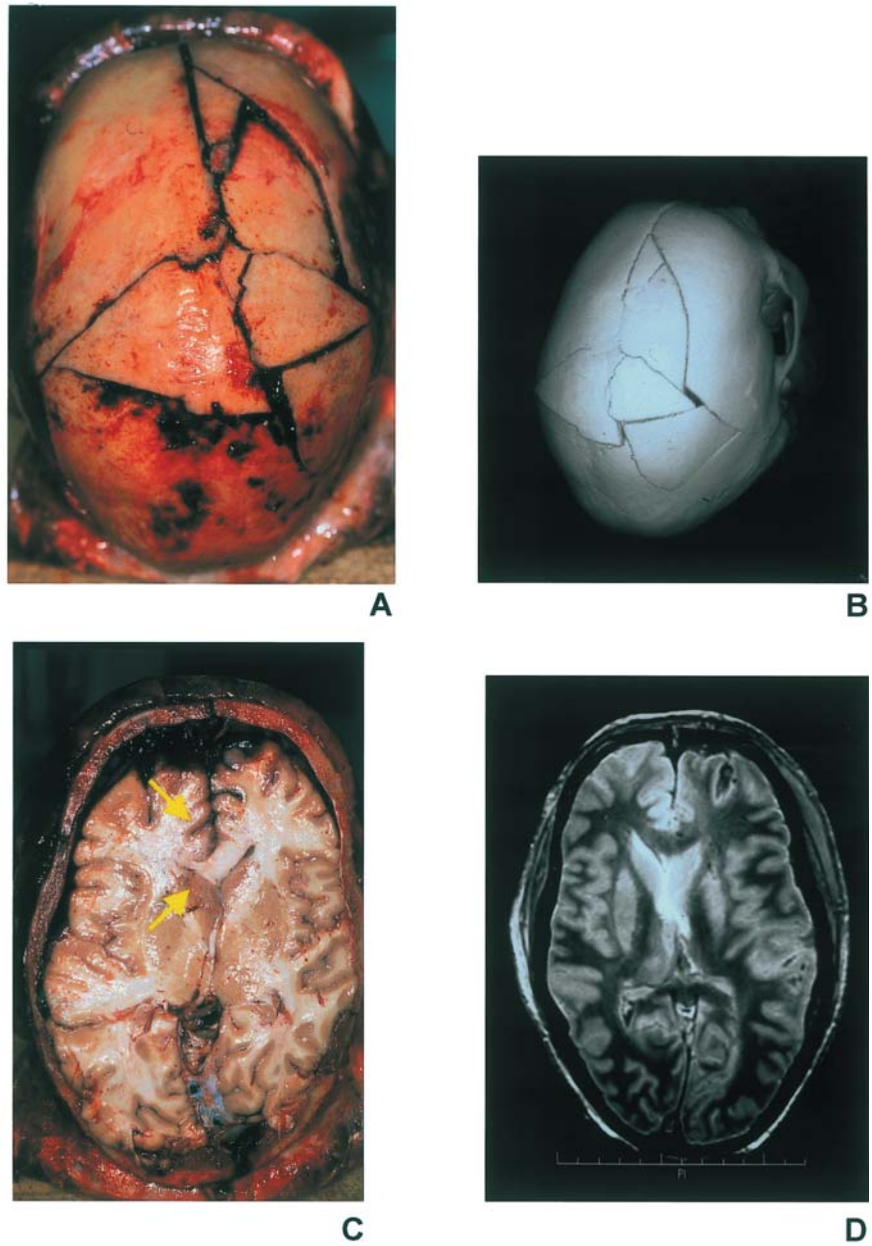

FIG. 1—*Burst fracture of the calvaria after blunt injury from a falling tree (Case 007)*: (a) *at autopsy*; (b) *corresponding 3D reconstruction (surface shaded display, 3D-SSD) from the CT data obtained before autopsy;* (c) *cranial view of brain after Flechsig cut—typical signs of elevated intracranial pressure such as compression of the anterior left ventricle, lateralization and subfalcian herniation with compression of the cingulated gyrus (arrows);* (d) *corresponding axial fast SE proton density MR image (3600/15), caudal view.*

Case 020 (Fig. 9*a* and 9*b*), we succeeded in demonstrating tension pneumothorax and air embolism. Competing causes of death were found in Cases 005 and 008, elevated ICP, air embolism, and hemorrhage in the former and simultaneous rupture of both heart and brainstem in the latter. The extent of hemorrhage as a possible cause of death was not evaluable by radiology (as mentioned above).

In conclusion, in trauma cases radiological diagnosis of the cause of death seems to yield more satisfying results than that of anatomo-pathologic ones. This is probably due to the circumstances that the "atria mortis" following trauma (aspiration, pneumothorax, air embolism, elevated ICP, organ rupture) are more readily demonstrated by imaging than the complex pathophysiological disturbances (multi-organ-failure, endocrinologic, or toxic metabolic disturbances) common in anatomo-pathological cases. Thus of the 47 partly combined causes of death found at autopsy, 26 (55%) were identifiable independently through radiological imaging. The only imaging clue to death by hemorrhage ($n = 13$) was aortic collapse (see above), while signs of cardiac failure ($n = 6$) or fat embolisms ($n = 2$) escaped detection by imaging altogether.

II. Traumatologic Findings

Skeletal System

Our results are on a par with others (2,3,7) in acknowledging the superiority of imaging techniques as compared to the conventional process of bone preparation by maceration. This advantage is illustrated exemplarily in cases of gunshot wounds (Cases 001, 011,

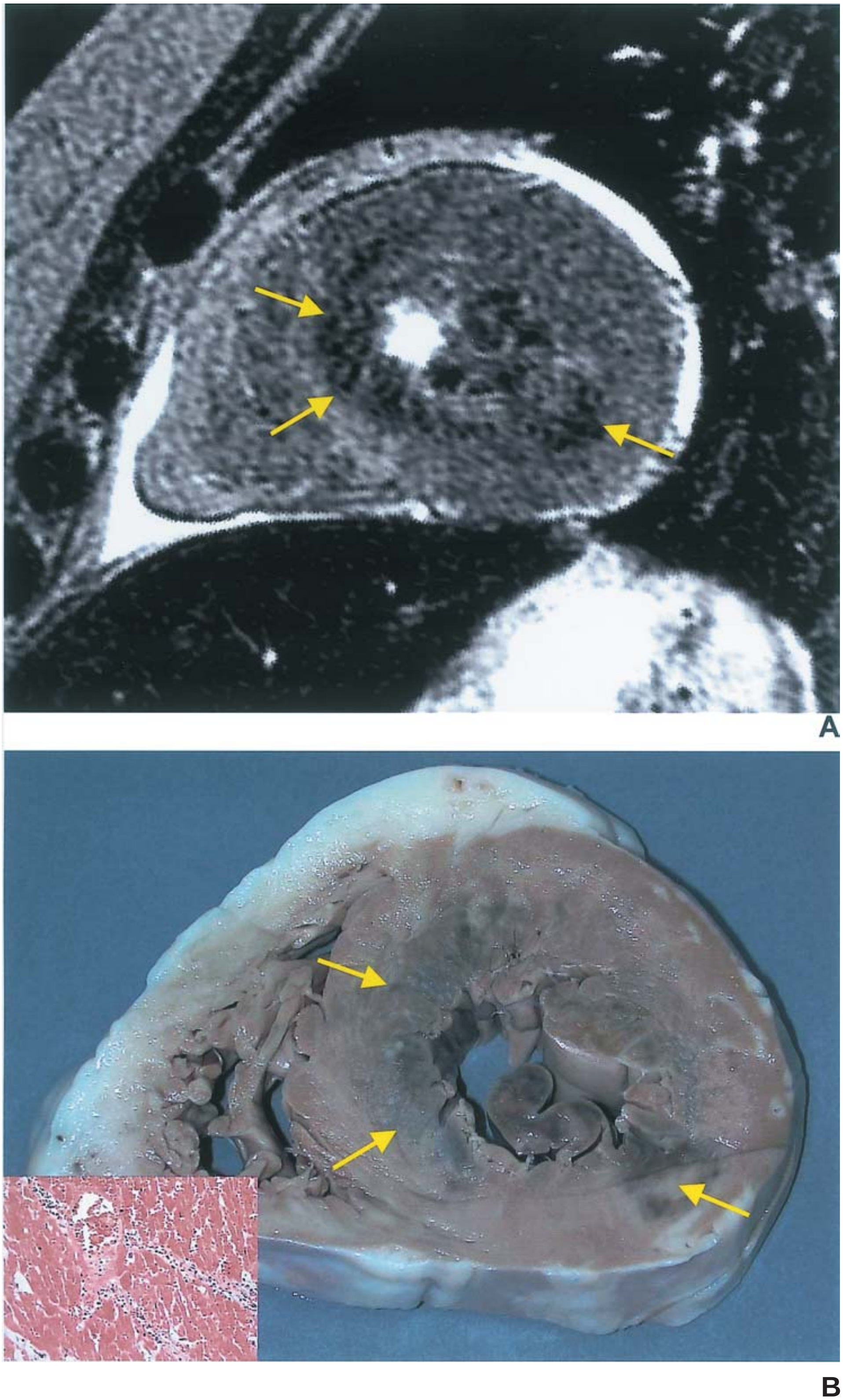

FIG. 2—*Recent myocardial infarction of the left ventricle (Case 013):* (a) *decreased signal intensity (arrows) in the subendocardial and partially transmural necrotic area; T2-weighted MR image (short axis, 3280/98);* (b) *autopsy and histological cuts showing scars combined with areas of acute myocardial infarction (arrows).*

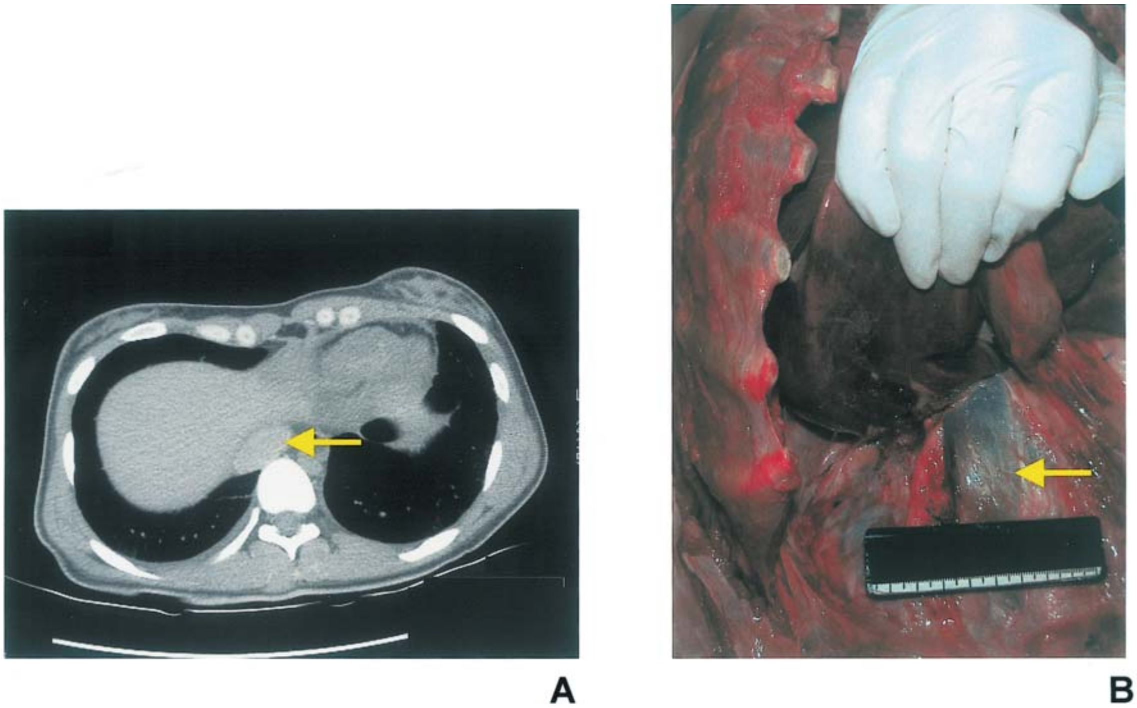

FIG. 3—*Death by drowning (Case 34):* (a) *axial CT image showing distension of the inferior vena cava (arrow) and engorgement of the systemic veins following right ventricular failure;* (b) *corresponding distension of the inferior vena cava at autopsy (arrow).*

012, 016, 021, 022, 031), burst fractures following blunt trauma (for example, Case 007, Fig. 1*a* and 1*b*) and fractures of the atlanto-occipital region (Cases 005, 023, 040).

At the same time, imaging is of great use in analyzing and visualizing complex fractures in inaccessible regions of the body, e.g., in fractures of facial bones. The face is usually exempt from dissection out of consideration for the relatives, and precise evaluation is hindered.

One study case was a corpse in advanced stage of decomposition (Case 027). Imaging clearly revealed skull fractures indicating homicide. The results delivered by MSCT/MRI were equivalent to those which conventional autopsy, followed by maceration, provides days, perhaps even weeks later.

In strangulation, the typical fractures of the hyoid bone (Case 032, Fig. 10*a–d*) were detected using radiology with precision and could even be distinguished from a contralateral anatomical variation (Fig. 10*a* and 10*b*).

Pelvic fractures, as seen in dashboard injuries (Case 020) or motorcycle/collision injuries (Cases 003, 018, and 035) also demonstrate the advantages of virtual versus conventional autopsy techniques. The possibility of precise 2D and 3D mapping of the fracture systems opens new avenues of research in the fields of biomechanics and motor vehicle safety. The traumatological data can be collected and correlated with data on bone density (juvenile versus osteoporotic bone).

The "Babygram" is another potential application for MSCT. In Case 024, a full-body MSCT scan provided an overview of the skeletal system.

Skin, Subcutaneous Fat, Muscle

These tissue layers are invaluable for the evaluation of impact location and force. An example is shown in Fig. 11*a* and 11*b* (Case 018) in which there had been direct vehicle impact contusion of the gluteal region following a bicycle accident. In order to judge the extent of damage to the layer of subcutaneous fat (hematoma or laceration), we used additional surface coils on the legs in Case 035 (MVA). Imaging allowed distinction between fatty tissue with hematoma only and crushed and lacerated subcutaneous fat.

Tissue hematoma after strangulation, even when slight as in Case 032, was successfully revealed using MRI (Fig. 10*c* and 10*d*). In cases of strangulation by a third party the lesions are more severe (28), so that we are optimistic about the abilities of MRI to reveal muscular hematoma in particular cases.

Internal Organs

MSCT or MRI proved very reliable in diagnosing cases of neurotrauma (15–17,29). In our study we had no difficulties in diagnosing epidural, subdural, and larger subarachnoid hemorrhage as well as contusion of the brain (coup-/contre-coup lesion). When taking into account the location and extent of accompanying scalp hematoma (Cases 019 and 028), determination of impact axis and vector—important in forensic reconstruction—posed no problems using radiological methods.

The least satisfying results were obtained diagnosing trauma to internal organs (kidney, spleen, liver, heart). As dynamic imaging and the application of contrast agents were not performed in our study cases, lesions were often invisible in imaging, particularly when death had occurred rapidly, leaving little or no hematoma at the site of injury. This is the domain in which the difference between postmortem and intravital radiological imaging was most striking. Nevertheless, in the case of a stab wound to the heart with ensuing hemopericardium, imaging provided a good result and diagnosis (Fig. 12*a–d*), because the stab wound was partly distended by a blood clot.

Further difficulties were encountered while rendering deep abdominal tissue trauma, which is of considerable forensic interest.

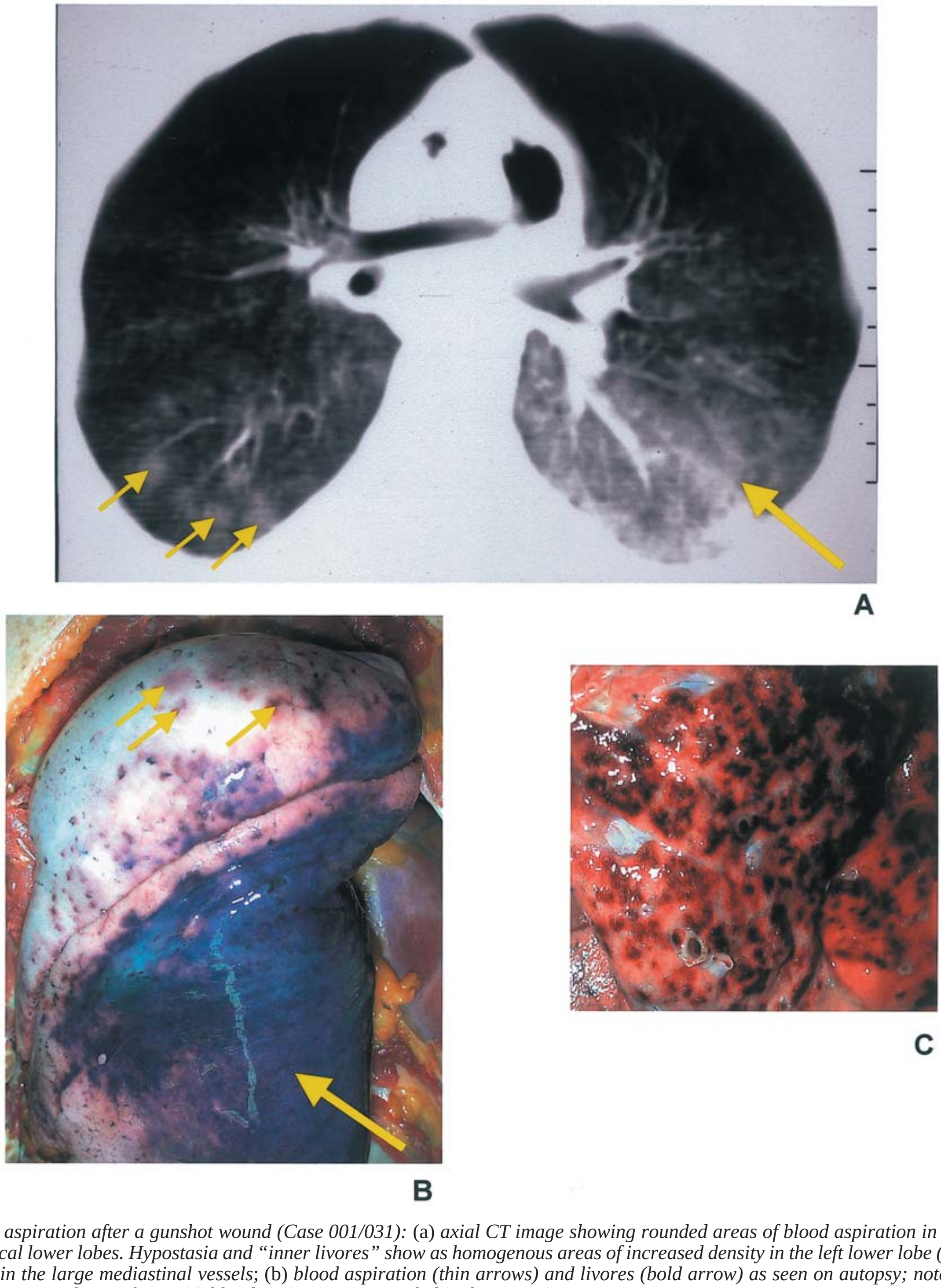

FIG. 4—*Blood aspiration after a gunshot wound (Case 001/031):* (a) *axial CT image showing rounded areas of blood aspiration in the right (thin arrows) and left apical lower lobes. Hypostasia and "inner livores" show as homogenous areas of increased density in the left lower lobe (bold arrow); note the air embolism in the large mediastinal vessels*; (b) *blood aspiration (thin arrows) and livores (bold arrow) as seen on autopsy; note the pallor of the parenchyma after massive hemorrhage;* (c) *blood aspiration as revealed in the autoptic cut.*

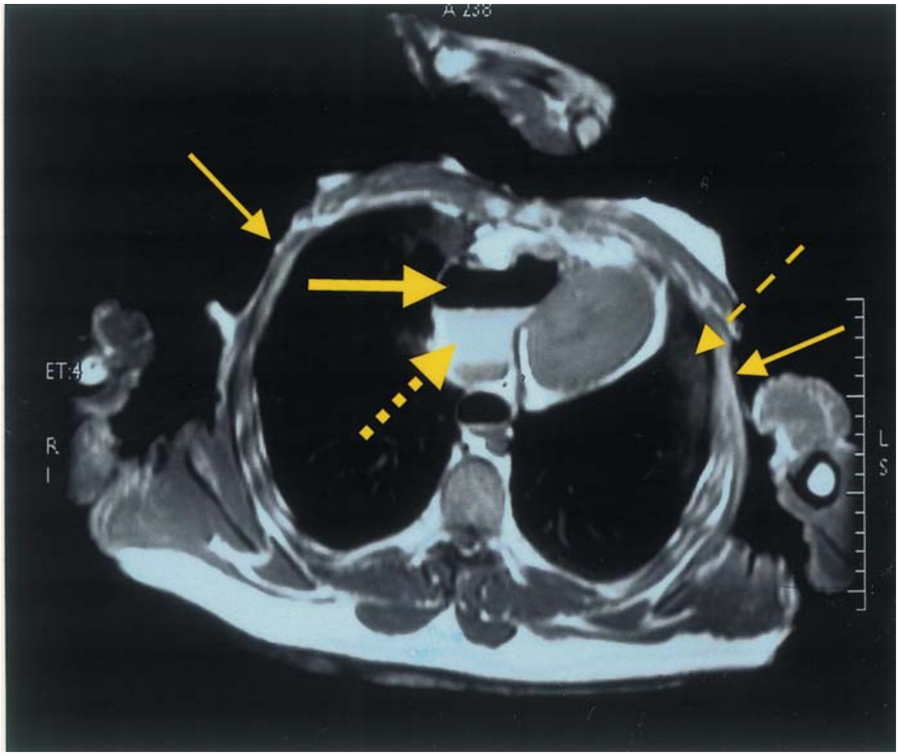

FIG. 5—*Burnt torso (Case 004). Varying degrees of carbonization as seen in the axial T1-weighted fast SE MR image (540/16). The ventral parts show partial loss of the signal-intensive layer of subcutaneous fat (thin arrows); contusion of the left lung (fragmented thin arrow); intracardial air embolism (bold arrow); trilayer sedimentation of blood components in the heart (fragmented bold arrow).*

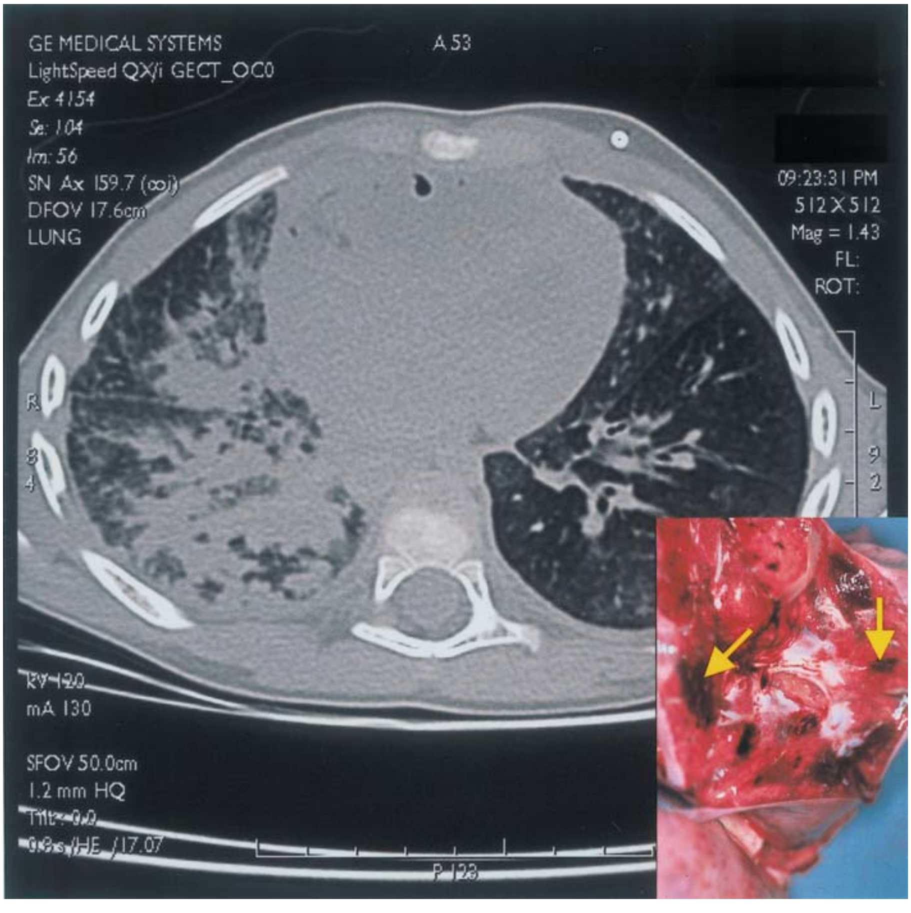

FIG. 6—*Aspiration of gastric acid (Case 009). Axial CT image showing partial lobular digestion of the lung parenchyma and atelectasis of the middle and inferior right lobes with isolated open bronchii. Inset: corresponding findings of lobular digestion at autopsy (arrows).*

Often contusion of the mesenteric root or compression and hematoma of the prevertebral, retroduodenal tissue is the only evidence left of blunt trauma to the abdomen (Cases 002, 005, 009, 015, 023).

III. Vital Reactions

Circulatory System

In our study the two foremost signs of continuing circulation after trauma, namely fat embolism and hemorrhage, were not traceable using MSCT/MRI imaging. They could only be deduced from other indirect signs such as the presence of a large amount of blood inside body cavities (Case 002). In these cases and in cases with stagnation of blood inside large vessels, we frequently observed a tri-layer separation of blood components (Fig. 5). It is yet unknown to what extent this layering reflects vital reactions or postmortem phenomena, as is the time at which separation occurs.

MSCT/MRI is much more sensitive than conventional autopsy in diagnosing air embolism (Fig. 13*a* and 13*b*) as a vital reaction. This is of particular value when anatomy is altered through scarring after inflammation (e.g., after cardiac bypass or transplant; valve replacement; pericarditis), and the application of the Richter test for cardiac air embolism is therefore hindered or made impossible (Case 021). Imaging of air embolism allows precise quantification and localization of air in heart, brain, liver, vessels, etc. (3,30–32).

In contrast, the effect of putrefaction on air content of organs requires further documentation and study. Preliminary results, however, indicate that the gaseous distension of organ cavities and parenchyma as putrefaction artifacts ("foam organs") can be diagnosed using imaging protocols (Case 027).

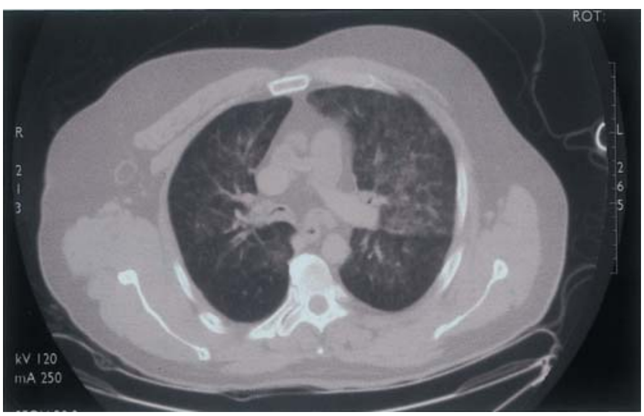

FIG. 7—*Emphysema aquosum after drowning (Case 039). Axial CT image showing patchy and blurred aspiration zones mainly in the left and ventral regions of the lung.*

Respiratory System

Cutaneous emphysema lends itself to radiological diagnosis. Similarily, pneumo-thorax is marked by both flattened diaphragm and air in the thoracic cavity. In the case of tension pneumothorax (Case 020), the mediastinal shift was documented only through imaging (Fig. 9*a*).

Aspiration is detected with high sensitivity using MSCT/MRI. More work is required, however, on identifying and differentiating the inhaled fluids (gastric juices, blood, water, stomach contents) and distinguishing radiological signs of aspiration from those of traumatic contusion and postmortem hypostasis.

IV. Forensic Reconstruction

In MVA, impact location and direction was identified in all victims (Cases 003, 008, 018, 035, 040; Fig. 11*a* and 11*b*) using radiological methods. In one case, the pattern of a complex cranial burst fracture indicated that the victim had been run over by the car (Case 015). Successful identification of impact axis and force in

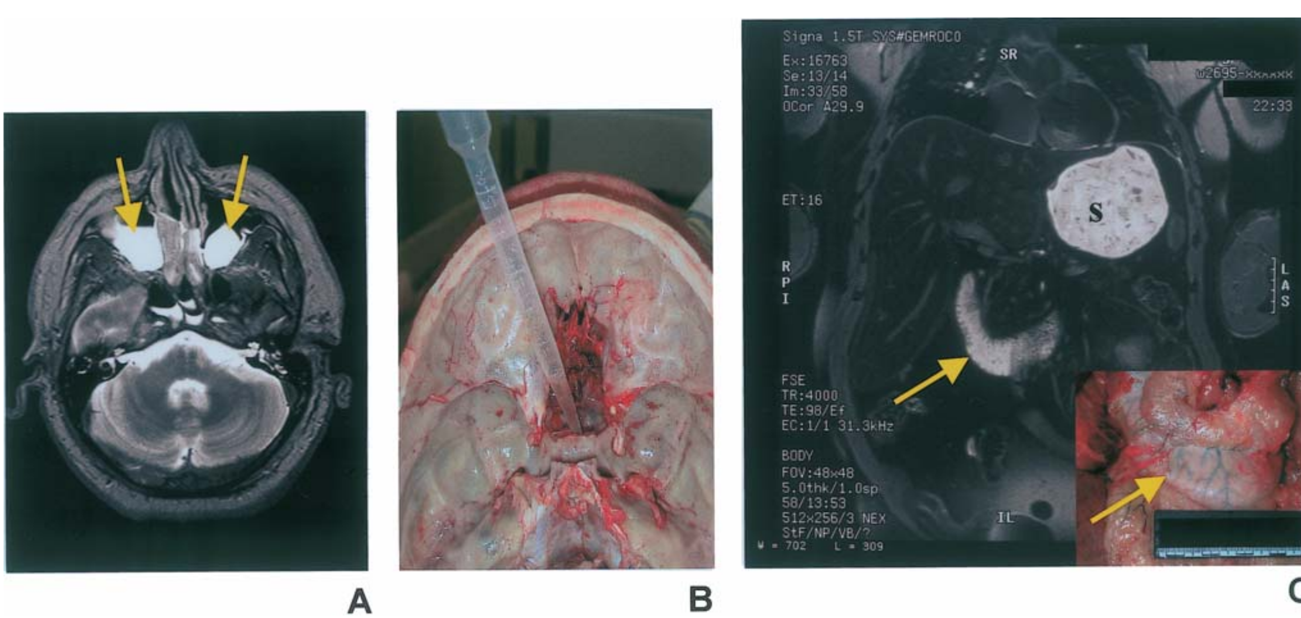

FIG. 8—*Drowning fluid as found in the paranasal cavities and intestinal tract (Case 034/039):* (a) *axial T2-weighted fast SE MR image (4000/105) showing both drowning fluid in parasnasal sinuses (arrows) and cerebrospinal fluid as signal–intensive areas;* (b) *aspiration of drowning fluid from the paranasal cavities during autopsy;* (c) *coronal T2-weighted fast SE fat-saturated MR image (4000/98) and inset from autopsy showing drowning fluid in both the stomach (s) and the duodenum (arrows), a forensic relevant vital reaction in drowning cases.*

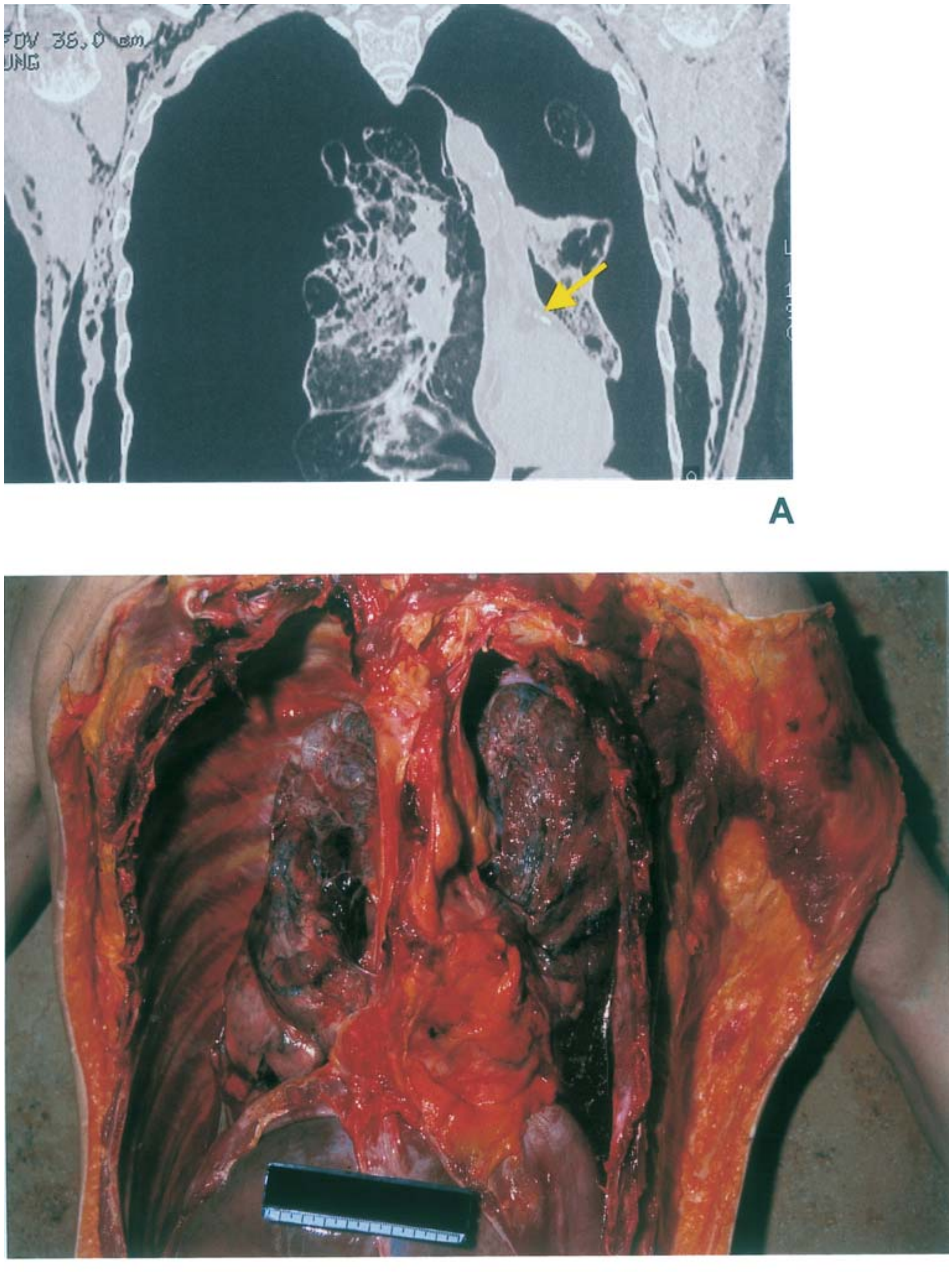

FIG. 9—Death after a motor vehicle accident (Case 020): (a) *pneumothorax with bilateral atelectasis and tissue emphysema; coronal MPR reconstruction from MSCT data shows the left-sided deviation of the mediastinum as proof of tension pneumothorax, which cannot be detected after opening the thoracic cavity in conventional autopsy; coronary artery calcification (arrow) as an incidental finding;* (b) *chest cavity at autopsy.*

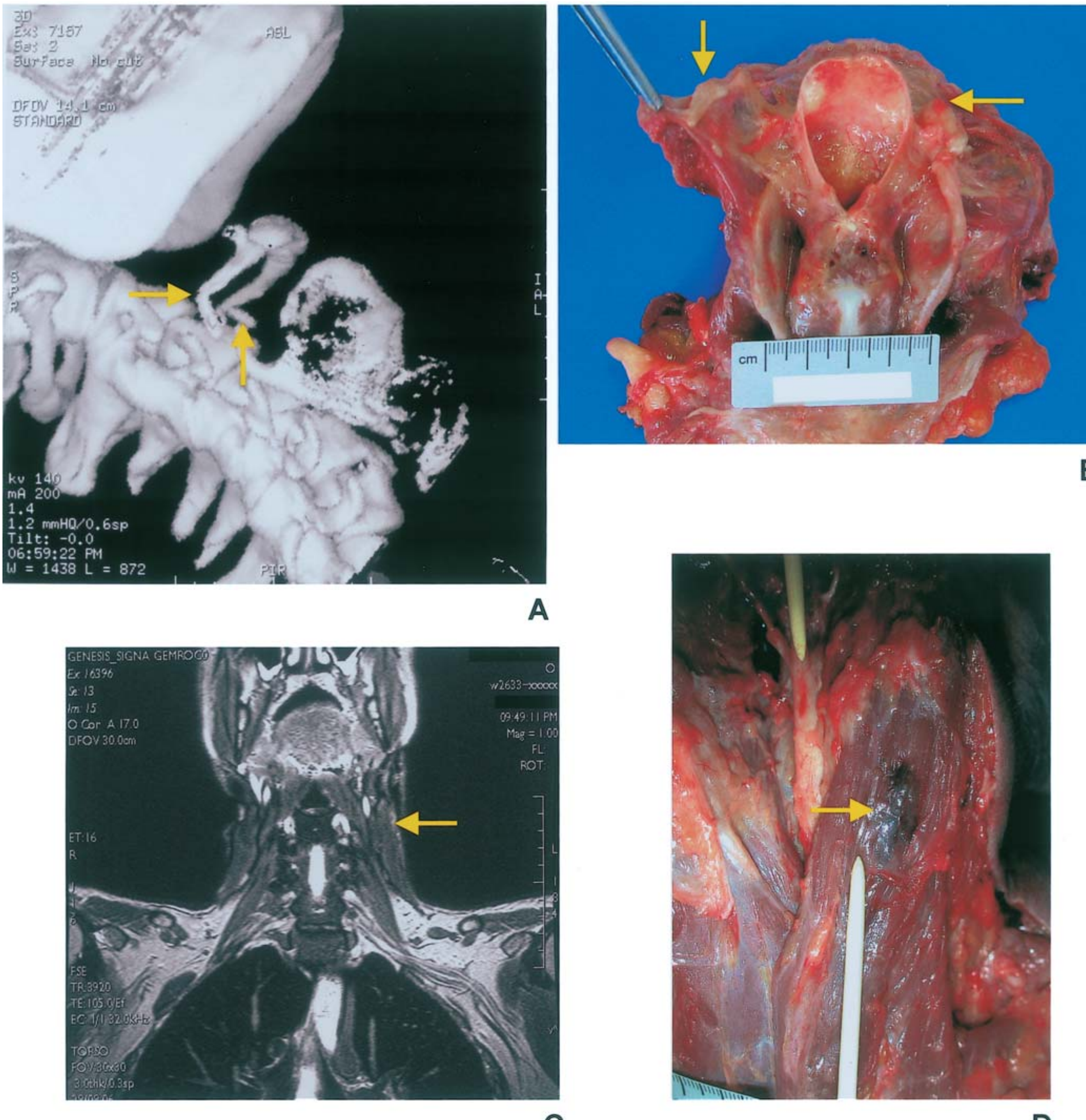

FIG. 10—*Death by hanging. Fracture of the right horn of the hyoid bone showing hematoma. Corpusculum triticeum (anatomical variation) on the left horn of the hyoid bone (Case 032)*: (a) *CT SSD-reconstruction; fracture (horizontal arrow) and corpusculum triticeum (vertical arrow);* (b) *dorsal view of the hyoid at autopsy; faint but visible hematoma at the fracture site (horizontal arrow); corpusculum triticeum on the left as shown in (a) (vertical arrow);* (c) *coronal T2-weighted fast SE MR image (3920/105) showing hematoma in the left musculus sternocleidomastoideus as a signal—intensive area (arrow);* (d) *corresponding area with hematoma during autopsy (arrow).*

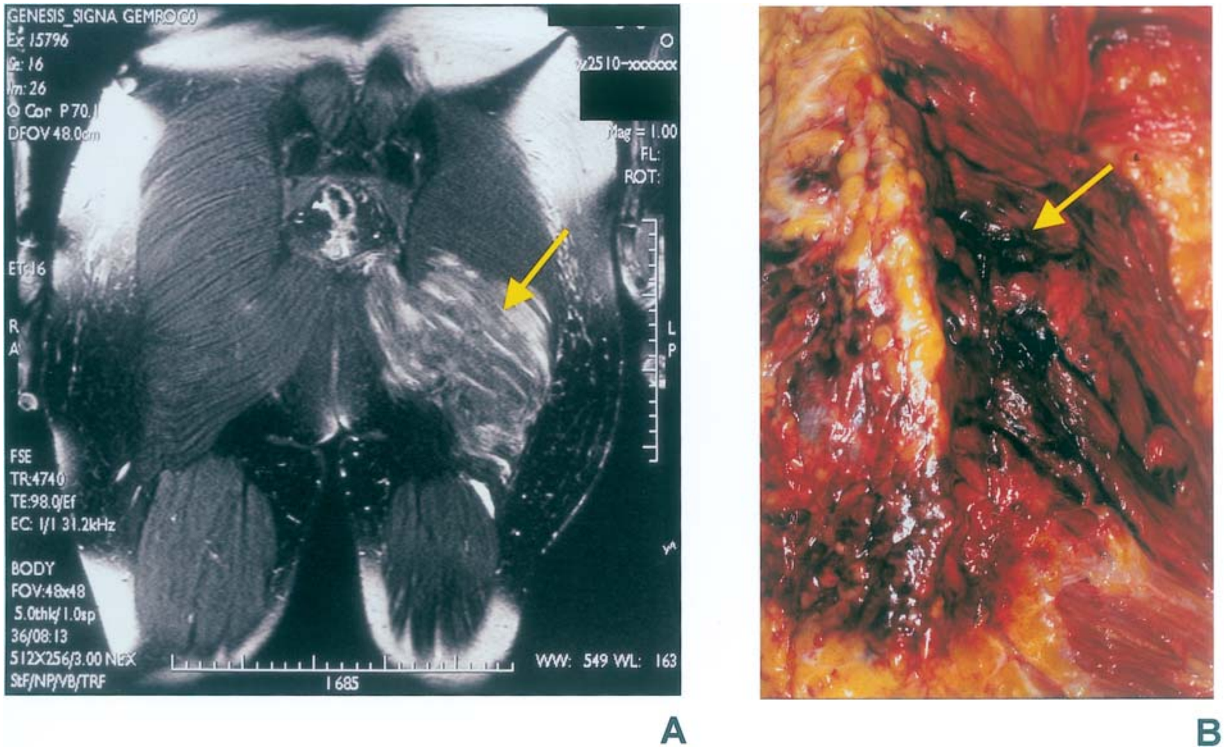

FIG. 11—*Contusion and hematoma of the right musculus glutaeus maximus after a bicycle/motor vehicle accident (Case 018):* (a) *coronal T2-weighted fast SE MR image (4740/98) showing the signal-intensive contusion zone (arrow);* (b) *corresponding area during the autopsy (arrow).*

cases of traumatic skull and brain injury (Cases 019 and 028) were already mentioned.

Imaging of ballistic injuries not only showed entry and exit wounds, but also—through analysis of fracture patterns—the order in which fractures occurred and the probable ammunition type. Bullet penetration of the tissues and ensuing wound canal were well documented using MSCT/MRI (Fig. 14*a* and 14*b*).

Wound depth and orientation in stabbings or slashings could be "guesstimated" using image data (Cases 030, 036).

In the burnt body (Case 004) we graded charring intensity of the tissues and could then deduce the direction of the flames (Fig. 5) based on radiological findings.

V. Visualization and Understanding of Forensic Results in the Court of Law

The enormous possibilities of 2D/3D image reconstruction and presentation using MSCT and MRI data are clearly superior to conventional, purely descriptive methods. Some findings such as firearm injuries and massive skull and extremities fractures are practically self-explanatory (Cases 001, 004, 005, 007, 011, 012, 016, 019, 020, 021, 022, 023, 027, 028, 029, 031, 033, 040). Image display is smooth and user-friendly, and the "unbloody" images are accessible and comprehensible to both laymen and experts in court.

Conclusions

The first systematic experiences while realizing our "virtopsy" project have demonstrated both the potential and the limitations of combined MSCT and MRI for the use of forensic science. For this kind of study it is absolutely necessary that there is a close interdisciplinary collaboration between the forensic pathologist and a radiologist. Postmortem imaging has one clear advantage and one major inconvenience as compared to clinical imaging: absence of motion artifacts allows optimal data acquisition, whereas lack of circulation and concomitant limits on the use of contrast agents will remain a problem in some cases. Innovative approaches such as protocol optimization and specific adaptation, the use of special coils, minimally invasive percutaneous biopsy, as well as sophisticated image processing might help to overcome these problems.

Based on our feasibility study we recommend performing MSCT first, using a rapid full-body screening in order to determine areas of particular forensic interest. There, MRI is used—when appropriate—where superior tissue contrast allows a detailed documentation of important organ and tissue findings. Due to the absence of motion artifacts, especially in MRI, and the fact that MSCT is not limited by radiation dose considerations, both methods produce images with excellent spatial resolution that sometimes even exceeds what is possible in clinical practice. Micro-CT techniques, Micro-MRI (MR microscopy) and postmortem angiography (33) could eventually occupy specific niches with regard to particular forensic questions. Finally, MR spectroscopy (MRS) combined with MRI could document preterminal and postmortem alterations in metabolite concentrations in tissues.

Documentation by radiological imaging is observer-independent, objective, and non-invasive. Digitally stored data may be recalled at will and provide fresh, intact topographical and anatomico-clinical reconstruction years after organic remains will have decayed and disappeared. Quality control and expert supervision become possible in a new manner, as well as image transmission and forensic "telemedicine" consultation. Image and data processing allows two- and three-dimensional views of forensic and anatomical findings, these reconstructed computed images allowing objective visualization and recapitulation of forensic results, MSCT with its high spatial resolution and quantitative density measurements, MRI allowing

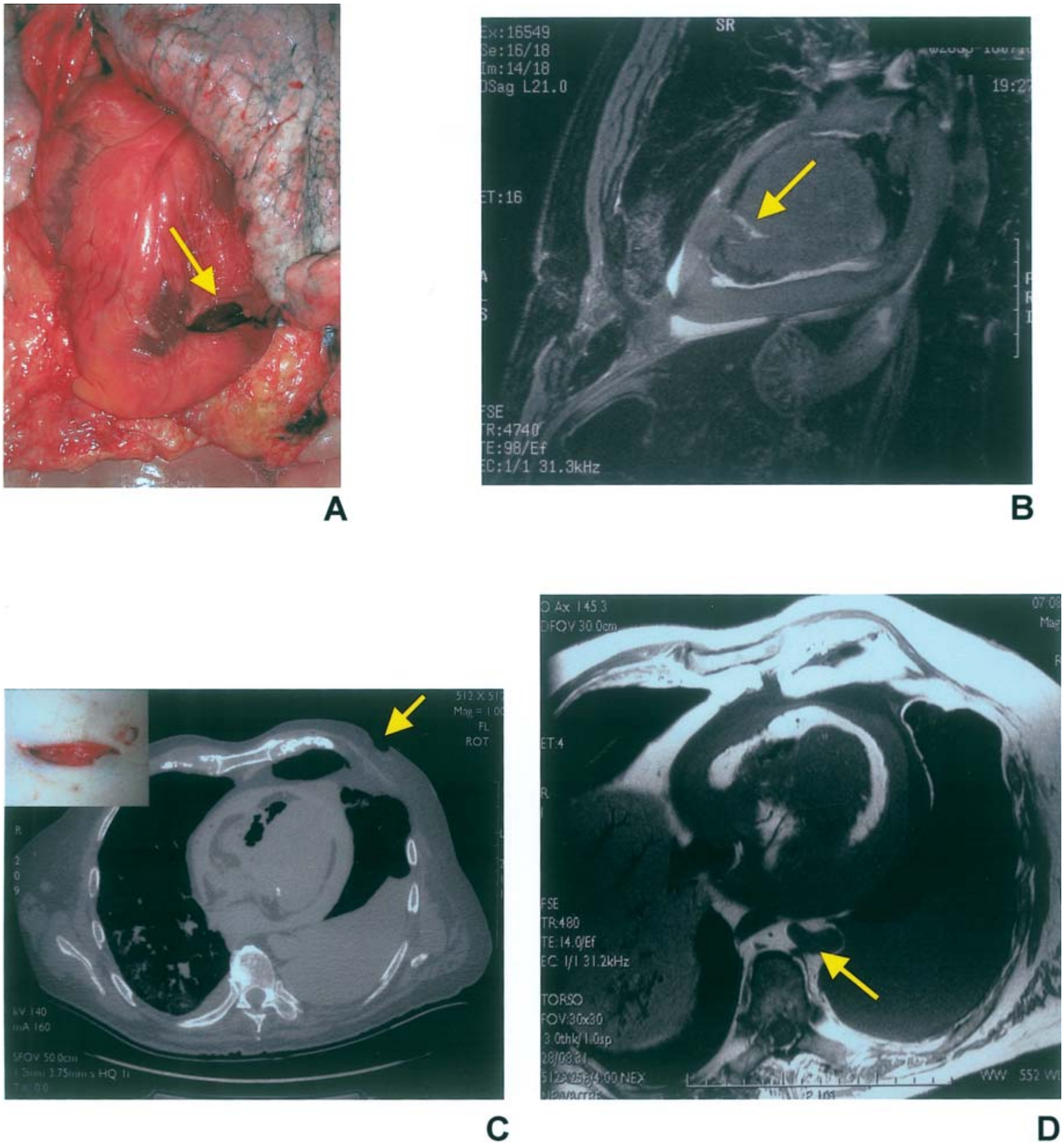

FIG. 12—*Self-inflicted stab wound to the heart (Case 036):* (a) *lesion of the ventricle as found during autopsy (arrow); (*b) *sagittal T2-weighted fast SE MR image (4740/98) showing penetration of the myocardium (arrow) with hemopericardium and intracardial blood clot;* (c) *skin lesion seen before autopsy (inset) and axial CT scan showing the skin defect (arrow) and the wound canal with hemopericardium, hemothorax, and intracardial air embolism;* (d) *corresponding axial T1-weighted fast SE MR image (480/14); clotting and hemopericardium are indicate of (short) survival time; the descending aorta (arrow) is collapsed following blood loss (c,d).*

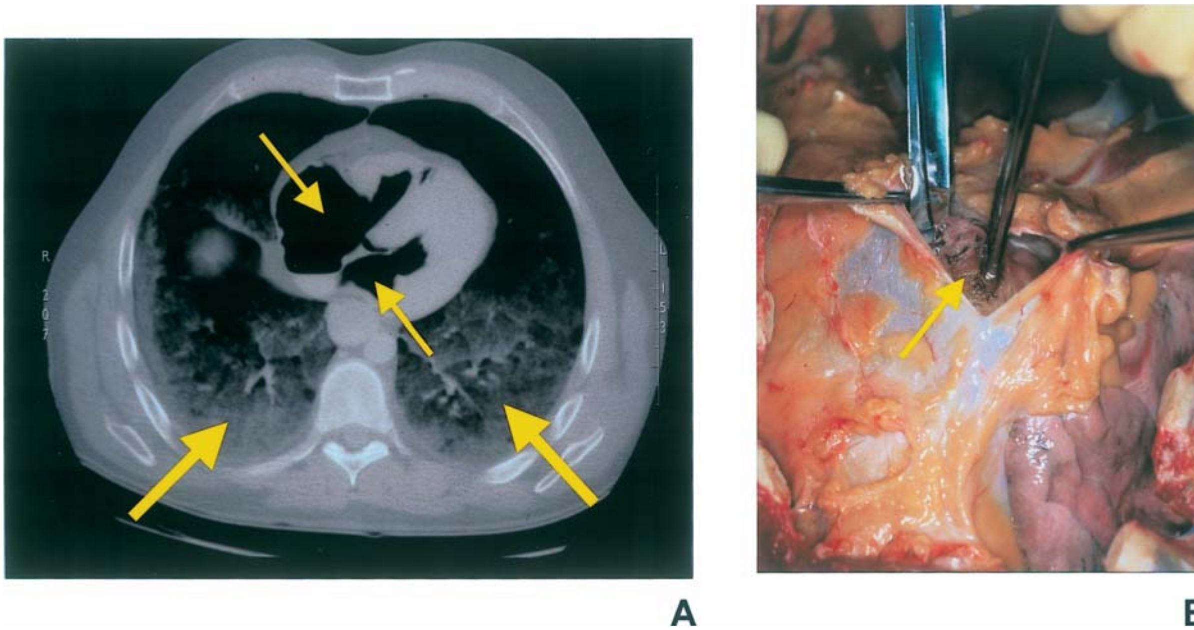

FIG. 13—*Suicidal gunshot wound of the head (Case 031):* (a) *biventricular air embolism (thin arrows) with patent foramen ovale; axial CT image also showing internal livores and hypostatical edema in both lungs (bold arrows);* (b) *Richter Test showing escaping air bubbles (arrow) after puncture of the right ventricle; this is the method conventionally used for demonstrating air embolism in the heart.*

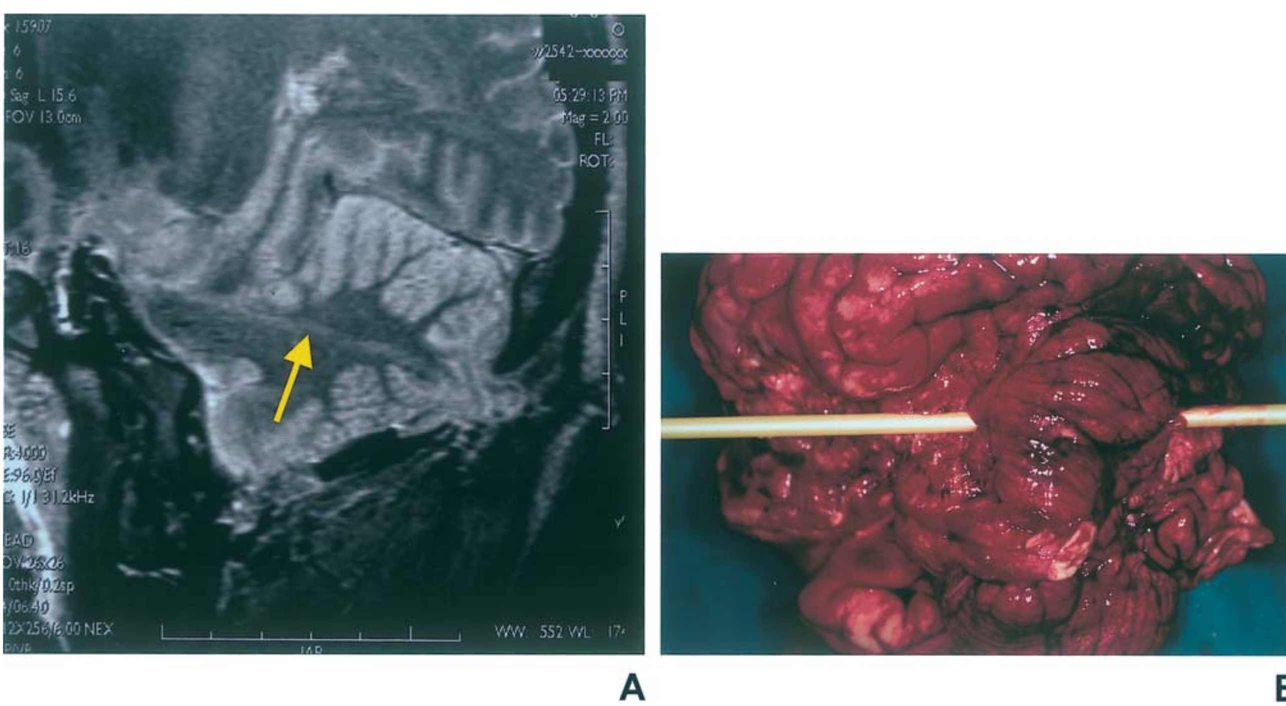

FIG. 14—*Gunshot wound (Case 022):* (a) *sagittal T2-weighted fast SE MR image (4000/96) showing the bullet track (arrow) through the cerebellum;* (b) *same bullet track marked with a probe during autopsy.*

tissue differentiation based on differential contrast weighting and—in the future—MRS with the possibility of metabolic-chemical analysis.

In certain cultural circles where conventional autopsy is stigmatized or even forbidden, virtual autopsy would allow sound medicolegal practice and support for the judicial system without violating religious prohibitions or personal reservations. Also, in the postmortem examination of highly infectious cadavers, this technique could be of particular use. Minimally invasive autopsy would reduce the number of conventional autopsies, which are often difficult to bear for relatives. This development could be similar to that observed with the advent of minimally invasive percutaneous or laparoscopic surgery.

The presented results of the feasibility study "virtopsy" project for radiologic evaluation of forensic cases are promising. The daily use of forensic radiological methods and future scientific studies in the forensic science will show whether these new diagnostic tools will augment or replace the classic autopsy procedure.

Based on our feasibility study, we hope that forensic-pathologic "know-how" combined with high-tech imaging will open new horizons in forensic medicine and other forensic sciences, leading towards a minimally invasive virtual forensic autopsy. Even more, however, the virtual reality of diagnostic radiology is entering the world of forensic pathology.

Acknowledgments

Particular thanks goes to the Gebert Ruef Foundation/Switzerland, without whose generous financial support the realisation of the first phase of the virtopsy project would not have been possible.

We thank Suzanne Horlacher, Elke Spielvogel, and Karin Zwygart (Department of Radiology, University of Berne) and also Roland Dorn and Urs Koenigsdorfer (Institute of Forensic Medicine, University of Berne) for the excellent help and data acquisition during the radiologic examination and the forensic autopsies.

Many thanks also to Barbara Ender and Cornelia Schwab (Department of Radiology/Institute of Forensic Medicine, University of Berne) and Paula Woodward (Armed Forces Institute of Pathology, Department Radiologic Pathology, Washington DC) for their radiologic and scientific support during this study; and to Nathalie Frickey for the translation.

References

1. Brodgon BG. Forensic radiology. Boca Raton: CRC Press, 1998.
2. Donchin J, Rivkind AI, Bar-Ziv J, Hiss J, Almog J, Drescher M. Utility of postmortem computed tomography in trauma victims. J Trauma 1994;37:552–6.
3. Farkash U, Scope A, Lynn M, Kugel C, Maor R, Abargel A, et al. Preliminary experience with postmortem computed tomography in military penetrating trauma. J Trauma 2000;48:303–9.
4. Harris LS. Postmortem magnetic resonance images of the injured brain: effective evidence in the courtroom. Forensic Sci Int 1991;50:179–85.
5. Hart BL, Dudley MH, Zumwalt RE. Postmortem cranial MRI and autopsy correlation in suspected child abuse. Am J Forensic Med Pathol 1996;17:217–4.
6. Nimkin K, Kleinman PK. Imaging of child abuse. Pediatr Clin North Am 1997;44:615–35.
7. Oliver WR, Chancellor AS, Soltys M, et al. Three-dimensional reconstruction of a bullet path: validation by computed radiography. J Forensic Sci 1995;40:321–4.
8. Wallace SK, Cohen WA, Stern EJ, Reay DT. Judicial hanging: postmortem radiographic, CT, and MR imaging. Features with autopsy confirmation. Radiology 1994;193:263–7.
9. Bisset R. Magnetic resonance imaging may be alternative to necropsy. BMJ 1998;317:1450.
10. Brookes JA, Hall-Craggs MA, Sams VR, Lees WR. Non-invasive perinatal necropsy by magnetic resonance imaging. Lancet 1996;348: 1139–41.
11. Niermeijer MF. Perinatal necropsy by magnetic resonance imaging. Lancet 1997;349:56.
12. Patriquin L, Kassarjian A, O'Brien M, Andry C, Eustace S. Postmortem whole-body magnetic resonance imaging as an adjunct to autopsy: preliminary clinical experience. J Magn Reson Imaging 2001;13:277–87.
13. Ros PR, Li KC, Vo P, Baer H, Staab EV. Preautopsy magnetic resonance imaging: initial experience. Magn Reson Imaging 1990;8:303–8.
14. Woodward PJ, Sohaey R, Harris DP, Jackson GM, Klatt EC, Alexander AL, et al. Postmortem fetal MR imaging: comparison with findings at autopsy. Am J Roentgenol 1997;168:41–6.
15. Harris J, Jr. The cervicocranium: its radiographic assessment. Radiology 2001;218:337–51.
16. Mattiello JA, Munz M. Four types of acute post-traumatic intracranial hemorrhage. N Engl J Med 2001;344:580.
17. Smith DH, Meaney DF, Lenkinski RE, Alsop DC, Grossman R, Kimura H, et al. New magnetic resonance imaging techniques for the evaluation of traumatic brain injury. J Neurotrauma 1995;12:573–7.
18. Hsu JCM, Johnson GA, Smith WM, Reimer KA, Ideker RE. Magnetic resonance imaging of chronic myocardial infarcts in formalin-fixed human autopsy hearts. Circulation 1994;89:2133–40.
19. Simonetti OP, Kim RJ, Fieno DS, Hillenbrand HB, Wu E, Bundy JM, et al. An improved MR imaging technique for the visualization of myocardial infarction. Radiology 2001;218:215–23.
20. Reeder SB, Du YP, Lima JA, Bluemke DA. Advanced cardiac MR imaging of ischemic heart disease. Radiographics 2001;21:1047–74.
21. Rossi SE, Goodman PC, Franquet T. Nonthrombotic pulmonary emboli. Am J Roentgenol 2000;174:1499–1508.
22. Schulthess GK, Schwitter J. Cardiac MR imaging: facts and fiction. Radiology 2001;218:326–8.
23. Stanford W. Coronary artery calcification as an indicator of preclinical coronary artery disease. Radiographics 1999;19:1409–19.
24. Boxt LM. Radiology of the right ventricle. Radiol Clin North Am 1999;7:379–400.
25. Sivit CJ, Taylor GA, Bulas DI, Kushner DC, Potter BM, Eichelberger MR. Posttraumatic shock in children: CT findings associated with hemodynamic instability. Radiology 1992;182:723–6.
26. Franquet T, Gimenez A, Roson N, Torrubia S, Sabate JM, Perez C. Aspiration diseases: findings, pitfalls, and differential diagnosis. Radiographics 2000;20:673–85.
27. Gluecker T, Capasso P, Schnyder P, Gudinchet F, Schaller MD, Revelly JP, et al. Clinical and radiologic features of pulmonary edema. Radiographics 1999;19:1507–31.
28. Lupetin AR, Hollander M, Rao VM. CT evaluation of laryngotracheal trauma. Semin Musculoskelet Radiol 1998;2:105–16.
29. Hayman JA, Taber KH, Ford JJ, Bryan RN. Mechanisms of MR signa alteration by acute intracerebral blood: old concepts and new theories. Am J Neuroradiol 1991;12:899.
30. Mirvis SE, Indeck M, Schorr RM, Diaconis JN. Posttraumatic tension pneumopericardium: the "small heart" sign. Radiology 1986;158:663–9.
31. Muth CM, Shank ES. Gas embolism. N Engl J Med 2000;342:476–82.
32. Oriscello RG, Robertello ME. CT scan demonstrating air in right ventricle. N Engl J Med 1993;328:855.
33. Saimanen E, Järvinen A, Penttilä A. Cerebral cast angiography as an aid to medicolegal autopsies in cases of death after adult cardiac surgery. Int J Legal Med 2001;114:163–8.

Additional information and reprint requests:
Richard Dirnhofer, M.D., Director
Institute of Forensic Medicine, University of Berne
IRM—Buehlstrasse 20
CH-3012 Berne, Switzerland
Phone: ++ 41 31 631 84 12
Fax: ++ 41 31 631 84 15
E-mail: dirnhofer@irm.unibe.ch